



HAL
open science

Estimation method for evaluating the wave-induced flicker level emitted by a tidal energy farm

Anne Blavette, Hamid Ben Ahmed, Bernard Multon, Lukas Morvan, Alice Verschae, Dara O 'Sullivan

► **To cite this version:**

Anne Blavette, Hamid Ben Ahmed, Bernard Multon, Lukas Morvan, Alice Verschae, et al.. Estimation method for evaluating the wave-induced flicker level emitted by a tidal energy farm. 11th European Wave and Tidal Energy Conference series (EWTEC), Sep 2015, Nantes, France. hal-01313219

HAL Id: hal-01313219

<https://hal.science/hal-01313219>

Submitted on 9 May 2016

HAL is a multi-disciplinary open access archive for the deposit and dissemination of scientific research documents, whether they are published or not. The documents may come from teaching and research institutions in France or abroad, or from public or private research centers.

L'archive ouverte pluridisciplinaire **HAL**, est destinée au dépôt et à la diffusion de documents scientifiques de niveau recherche, publiés ou non, émanant des établissements d'enseignement et de recherche français ou étrangers, des laboratoires publics ou privés.

Estimation method for evaluating the wave-induced flicker level emitted by a tidal energy farm

Anne Blavette, Hamid Ben Ahmed, Bernard Multon
SATIE (CNRS)
Ecole Normale Supérieure-Rennes
France
E-mail: anne.blavette@ens-rennes.fr

Lukas Morvan, Alice Verschae
Ecole Navale
(French Naval Academy)
France

Dara O'Sullivan
Analog Devices
Cork
Ireland

Abstract—The inherently fluctuating nature of sea waves can be reflected to a significant extent in the power output of tidal turbines. However, these fluctuations can give rise to power quality issues such as flicker. Hence, it is important to assess the impact which tidal farms may have on their local network before such power plants are allowed to connect to the grid. This paper analyses under which sea-state and grid conditions a 30 MW rated tidal farm breaches the grid code requirements in terms of short-term flicker level. Then, it describes a simplified method for estimating the flicker level by means of an equivalent sinusoidally-modulated voltage profile.

Index Terms—Tidal turbine, flicker, wave, impedance angle, device number

I. INTRODUCTION

Tidal turbines are now considered as sufficiently mature to be deployed in pre-commercial tidal farms [1], [2]. So far, they have been tested in sheltered areas where the influence of sea waves on their power output could be considered as negligible [3]. Hence, the flicker level generated by tidal turbines subject to the influence of waves has not been analysed experimentally, nor has it been studied numerically. However, the wave power fluctuations can be reflected to a significant extent on the electrical power output of a tidal turbine [4]. This paper intends to fill this gap by evaluating the flicker level generated by a tidal farm by means of numerical power system simulations. It will also detail a simplified method for estimating the flicker level generated by a tidal farm under the action of waves.

II. MODELING

A. Tidal Turbine Characteristics

The characteristics of the tidal turbine considered in this study were extracted from [4] and are summarized in Table I. The turbine is equipped with a permanent magnet synchronous generator. However, contrary to [4], no supercapacitor banks are included in the electrical conversion chain, which constitutes a worst case scenario.

B. Modeling of the Horizontal Water Speed

The mechanical power extracted by a tidal turbine is calculated based on the horizontal component U of the water flow speed perpendicular to the rotation plane of its blades. This horizontal speed is composed of contributions from the tidal current and from the waves. These two phenomena are

Parameter	Value
Turbine blade radius	8 m
System total inertia	1.3131×10^6 kg.m ²
Turbine rated power	1.5 MW
Pole pair number	120
Permanent magnet flux	2.458 Wb
Generator stator resistance	0.0081 Ω
Generator d - q inductance	1.2 mH
Grid frequency	50 Hz

TABLE I
CHARACTERISTICS OF THE CONSIDERED TIDAL TURBINE (EXTRACTED FROM [4])

coupled as a tidal current of significant speed may result in a non-negligible increase of the mean wave height [5]. However, this coupling is usually neglected even for detailed turbine structural design analyses [6]. Hence, it was deemed reasonable for the power system simulations performed in this study not to model these interactions, in similar fashion to [4]. Consequently, the horizontal component U of the water flow speed at any point in space and time can be formulated as

$$U(x, z, t) = U_t(x, z, t) + U_w(x, z, t) \quad (1)$$

where x is the coordinate of the horizontal axis (which is parallel to a supposedly flat sea bottom), z is the coordinate of the vertical axis (which is perpendicular to the sea bottom), t is the time, U_t and U_w are the speed contributions from the tidal current and from the waves respectively. It should be noted that the speed contributions U_t and U_w are collinear which constitutes the most unfavorable case.

1) *Tidal current contribution U_t* : The tidal flow is considered as linear and perpendicular to the rotation plane ($0yz$) of the turbine blades. Hence, no turbulence effect is considered in this study. It is important to recall that, although this phenomenon may induce a significant level of flicker [3], the objective of this study consists in analysing wave-induced flicker only. The variations of the tidal flow speed $U_t(z, t)$ at the sea surface ($z=0$ m) as a function of time is usually considered as sinusoidal such as

$$U_t(x, 0, t) = \max[U_t(x, 0, t)] \sin\left(\frac{2\pi t}{T_t}\right) \quad (2)$$

where $\max[U_t(x, 0, t)]$ is the maximum tidal current speed selected arbitrarily as equal to 3.5 m/s in this study. This value is typical of high speed tidal currents characterising the areas where tidal farms are envisaged to be deployed. Term T_t is the tidal period which is almost equal to half a lunar day, i.e. $12h25 \approx 44,700$ seconds. The variations of the tidal flow speed as a function of the water depth z ($z < 0$) can be modeled as follows [7]

$$U_t(x, z, t) = U_t(x, 0, t) \left(\frac{d+z}{d} \right)^{\frac{1}{7}} \quad (3)$$

where d is the distance between the sea surface and the sea bottom which is equal to 35 m in this study. This water depth corresponds to this of the site selected for the Paimpol-Bréhat tidal farm in France [4]. In summary, the contribution in speed $U_t(x, z, t)$ from the tidal current can be expressed as

$$U_t(x, z, t) = \max[U_t(x, 0, t)] \sin \left(\frac{2\pi t}{T_t} \right) \left(\frac{d+z}{d} \right)^{\frac{1}{7}} \quad (4)$$

2) *Waves contribution U_w* : The speed contribution U_w due to waves is usually modeled based on the linear wave theory [8]. However, this theory is not valid for shallow to intermediate waters which are traditionally characterised by a water depth less than 50 m, as it is the case in this study. Stokes wave theory is the typical alternative for modeling non-linear waves in shallow to intermediate waters. The order of the Stokes law must be selected based on the water depth d and on the characteristics of the wave climate considered. Considering that a classical Bretschneider spectrum was selected, these wave climate characteristics consist of the significant wave height H_s and of the peak period T_p .

In this study, the significant wave height range considered is $2 \text{ m} \leq H_s \leq 8 \text{ m}$ and the peak period range considered is $5 \text{ s} \leq T_p \leq 15 \text{ s}$. These values correspond to wave climates having low to high energy levels. It appears clearly from Fig.1 that, under the conditions considered in this paper, waves can be modelled according to the 2nd order Stokes law. Consequently, the velocity potential Φ at depth z due to a monochromatic wave of height H and of period T can be expressed as [9]

$$\Phi = \frac{HL}{2T} \frac{ch(k(d+z))}{sh(kd)} \sin(kx - \omega t) + \frac{3\pi^2 H^2}{16T} \frac{ch(2k(d+z))}{sh^4(kd)} \sin(2(kx - \omega t)) \quad (5)$$

where L is the wavelength, k is the wave number defined as $k = 2\pi/L = \omega/\sqrt{gd}$ [8], ω is the radian frequency and g is the gravitational acceleration. Hence, the speed contribution U_{w_i} of a single monochromatic wave on the Ox axis (parallel to the supposedly flat sea bottom) can be calculated as

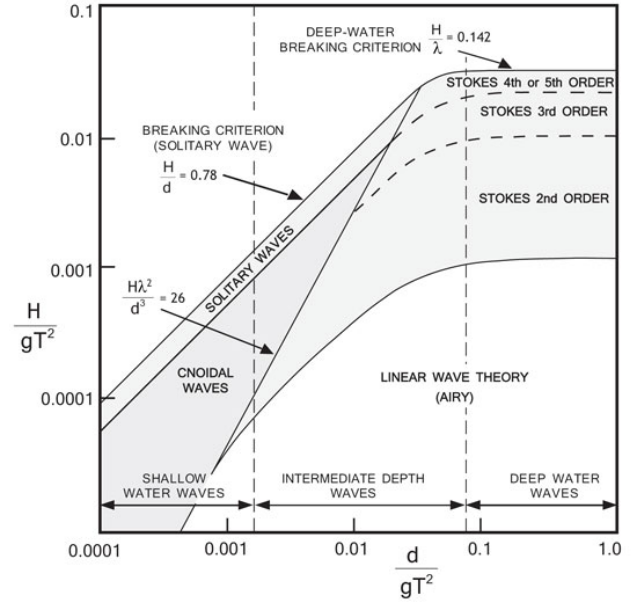


Fig. 1. Domain of validity of different hydrodynamic theories (after [10])

$$U_{w_i}(x, z, t) = \frac{d\Phi}{dx} = \frac{\pi H}{T} \frac{ch(k(d+z))}{sh(kd)} \cos(kx - \omega t) + \frac{(3\pi^2 H^2)}{4TL} \frac{ch(2k(d+z))}{sh^4(kd)} \cos(2(kx - \omega t)) \quad (6)$$

However, a sea-state is the sum of multiple waves of amplitude a_i , of period T_i , of wave number k_i and of random phase ϕ_i (in this paper, all the random phases ϕ_i are assumed to be equal to zero, which represents a worst case scenario). Hence, the horizontal speed U_w of the water flow due to the action of waves is equal the sum of the speed contributions U_{w_i} corresponding to all the monochromatic waves:

$$U_w(x, z, t) = \sum_i U_{w_i}(x, z, t) = \sum_i \frac{2\pi a_i}{T_i} \frac{ch(k_i(d+z))}{sh(k_i d)} \cos(k_i x - \omega_i t + \phi_i) + \frac{3\pi^2 a_i^2}{T_i L_i} \frac{ch(2k_i(d+z))}{sh^4(k_i d)} \cos(2(k_i x - \omega_i t + \phi_i)) \quad (7)$$

The amplitudes a_i are calculated such as [8]

$$a_i = \sqrt{2S(f_i)\Delta f} \quad (8)$$

C. Averaged Water Flow Speed

As it will be explained in the next section, the mechanical power extracted by the tidal turbine depends on the cube of the water flow speed $U(t)$ averaged over the circular surface swept by the blades. This averaged flow speed can be calculated as

$$\langle U(t) \rangle = \frac{\int_{-d_h-R}^{-d_h+R} U(x, z, t) 2\sqrt{R^2 - (d_h + z)^2} dz}{\pi R^2} \quad (9)$$

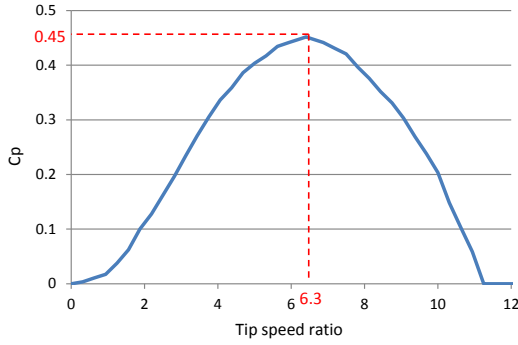


Fig. 2. C_p coefficient as a function of the tip speed ratio (after [4])

where d_h is the sea depth at which the hub of the tidal turbine is located (here $d_h=22$ m) and R is the turbine blade radius equal to 8 m, as already indicated in Table I.

Profiles for the averaged speed $\langle U(t) \rangle$ were simulated for four values of the significant wave height H_s : 2 m, 4 m, 6 m, 8 m, and for four values of the peak period T_p : 5 s, 7 s, 9 s, 11 s, 13 s, 15 s.

D. Modeling of the Tidal Turbine

The mechanical power $P_{mec}(t)$ extracted by the tidal turbine can be expressed as

$$P_{mec}(t) = \frac{1}{2} C_p \rho \pi R^2 \langle U(t) \rangle^3 \quad (10)$$

where C_p is the power coefficient and ρ is the density of sea water equal to 1027 kg/m^3 . The curve of the optimal power coefficient C_p as a function of the tip speed ratio λ considered in this study was extracted from [4] and is reproduced in Fig 2. The tidal turbine is controlled in speed so that the power coefficient C_p remains sufficiently close to its maximal value. The control system was developed under Matlab-Simulink and is shown in Fig. 3. The mechanical power $P_{mec}(t)$ extracted by the tidal turbine is computed based on the rotor speed and on the C_p - λ characteristic of the turbine in the “Power extraction” block. This block computes also the dynamic reference speed $\omega_{ref}(t)$ to maintain power coefficient C_p close to its maximal value. The error between the dynamic reference speed $\omega_{ref}(t)$ and the rotor speed is transformed into voltages to be applied at the terminals of the turbine. The blocks “dq2abc” and “PWM inverter” were extracted from Simulink model “power_pmmotor.mdl” and simulate field-oriented control [11]. The d - q axes inductances L_d and L_q are equal and the generator has permanent magnet excitation so the control of the electrical torque relies solely on the quadrature axis current i_q . The direct axis current i_d is maintained at zero.

E. Modeling of the Tidal Farm

The electrical power output $P_{tot}(t)$ of an entire tidal farm composed of 20 turbines was simulated based on the addition of identical individual electrical power profiles $P_{e_n}(t)$ (where

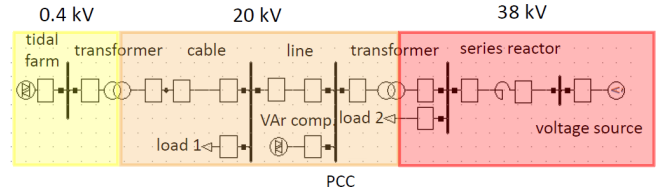


Fig. 4. Electrical network to which the tidal farm is connected. The reactor in series with the constant voltage source represents the rest of the national network.

$n=\{1, \dots, 20\}$), each shifted by a random time delay δ_n [12]. This enables to simulate the aggregation effect of several devices subject to the action of waves with a reduced computing time compared to simulating the power output profile of each tidal turbine. Although this method does not enable to include the effect of wave dispersion, it is assumed that this has a negligible impact on the flicker level generated by the tidal farm. The tidal turbines are assumed to be operated at unity power factor, thus leading to a farm nominal power S_n equal to $20 \times 1.5 = 30$ MVA.

F. Modeling of the Electrical Network

The electrical network was modeled under power system simulator PowerFactory [13] as shown in Fig. 4. It is composed of (from right to left): a “static generator” built-in model outputting the electrical power output $P_{tot}(t)$ of the tidal farm, a 0.4/10 kV transformer, a 1 km long submarine cable whose length was selected arbitrarily and whose impedance is equal to $0.10+j0.12 \ \Omega$, a 0.1 MVA load (load 1), a 5 km long overhead line whose impedance is equal to $0.45+j1.50 \ \Omega$, a VAr compensator maintaining the power factor at the point of common coupling (PCC) at unity, a 20/38 kV transformer, a 2 MVA load (load 2) and finally a $15 \ \Omega$ impedance in series with a constant 38 kV voltage source simulating the rest of the national grid. This last impedance corresponds to a short-circuit level equal to 96 MVA which is representative of average coastal networks. Four values of the impedance angle Ψ_k were considered: 30° , 50° , 70° , 85° , as recommended in IEC standard 61400-21 [14]. This network model is inspired from another already used in previous works [15] and representing the Irish marine energy test site, called AMETS, located off Belmullet [16]. Short-term flicker was evaluated by means of a flickermeter compliant with IEC standard 61000-4-15 [17].

III. RESULTS

A. Compliance with Grid Code Requirements

Fig. 5 shows the flicker level corresponding to different wave heights H_s , to different peak periods T_p and to different impedance angles Ψ_k . It appears clearly that the tidal farm complies with the most permissive flicker requirement ($P_{st,max}=1$) enforced in a number of national grid codes [15] under any conditions. The tidal farm complies also with the most stringent limit ($P_{st,max}=0.35$) except for relatively resistive grids (i.e. low impedance angle Ψ_k) and storm conditions ($H_s \geq 8$ m) during which the tidal turbines would

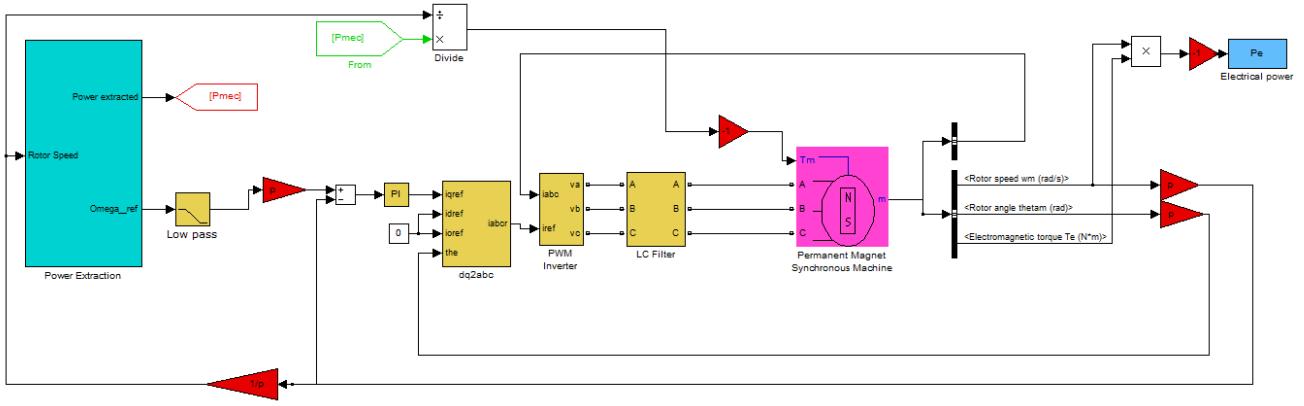


Fig. 3. Tidal turbine model developed under Matlab-Simulink

not be operated anyway. Hence, it can be concluded, under the conditions considered here, that flicker issues are unlikely to appear due to the grid connection of a middle-sized tidal farm only.

However, the flicker level induced by the tidal farm may be far from being negligible. Consequently, the total flicker level may exceed the maximum allowed limit at the PCC in case other installations connected at the same node induce flicker as well. Hence, it is important to assess the level of flicker induced by a tidal farm. However, flicker analyses are often time-consuming and require knowledge on potentially confidential commercial data which tidal turbine developers may not be willing to provide. Consequently, flicker analyses are only performed, if they are at all, at the final stage of the grid connection process, despite the potentially very negative consequences of poor power quality from a technical, economical and human point of view.

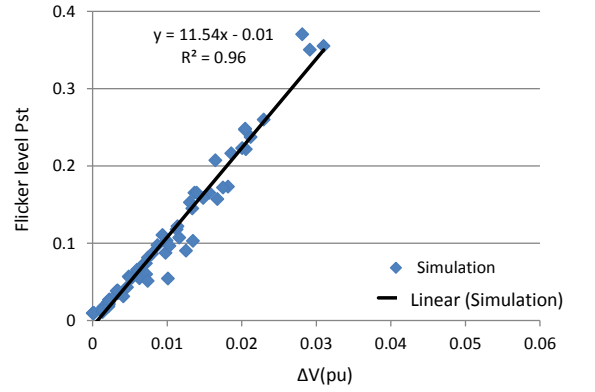
It is in this context that a simplified method was developed to estimate the flicker level induced by a tidal farm subject to the action of waves. This method relies on two points: 1) the relation of linearity existing between the flicker level P_{st} and the maximum voltage difference ΔV characterising a voltage profile, 2) the existence of a sinusoidally-modulated voltage profile equivalent in terms of flicker to any voltage profile induced by a tidal farm on its local network. Both these points, as well as the method itself, are described in the following sections.

B. Linear Relation between the Flicker Level P_{st} and the Maximum Voltage Difference ΔV

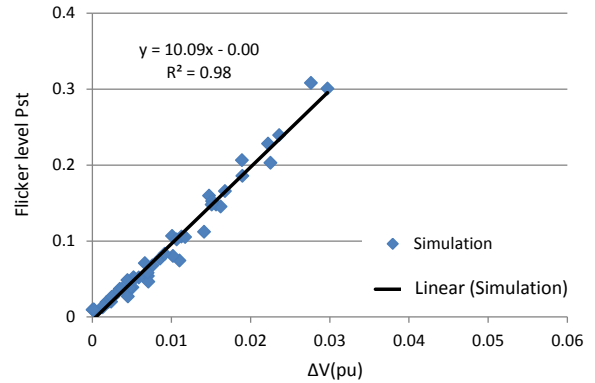
There exists a linear relation between the flicker level P_{st} and the maximum voltage difference $\Delta V = \max(V(t)) - \min(V(t))$ corresponding to a given voltage profile $V(t)$ induced by a wave farm on its local network [15]. This is also valid in the case of a tidal farm subject to the action of waves, which is confirmed by the results of the power system simulations shown in Fig. 6.

In summary, it can be stated that

$$P_{st} \approx a\Delta V \quad (11)$$



(a) $T_p = 5 \text{ s}$



(b) $T_p = 7 \text{ s}$

where coefficient a is independent of the impedance angle Ψ_k and of the significant wave height H_s , but depends on the peak period T_p .

C. Equivalent sinusoidally-modulated voltage profile

Equation (11) implies that there exists sinusoidally-modulated voltage profiles $v_{eq}(t)$ which are equivalent, in

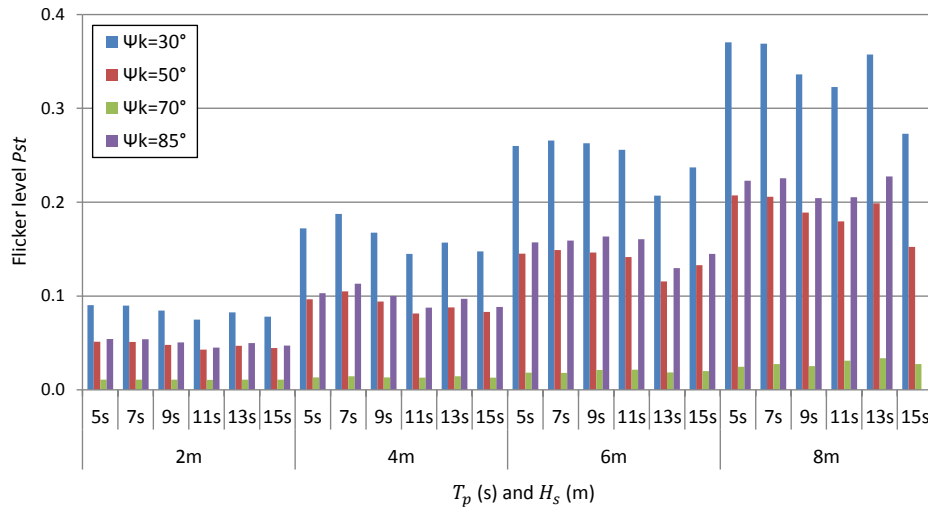
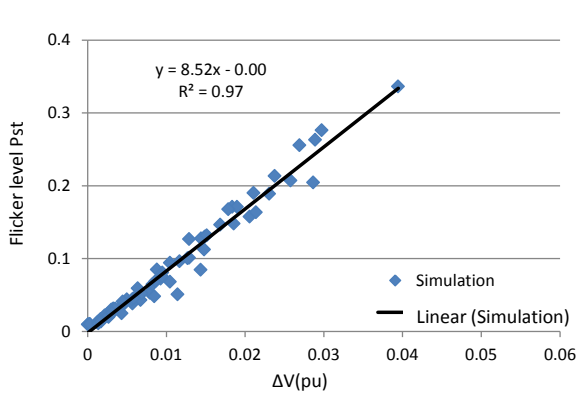
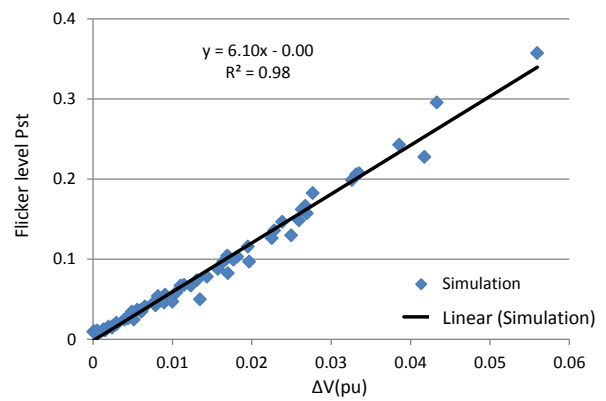


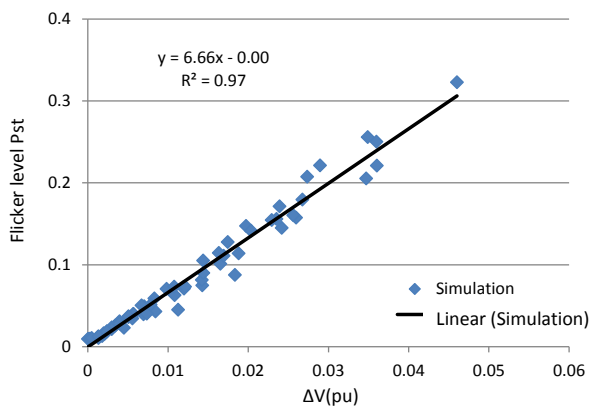
Fig. 5. Flicker level P_{st} as a function of the peak period T_p and of the significant wave height H_s for different impedance angles Ψ_k .



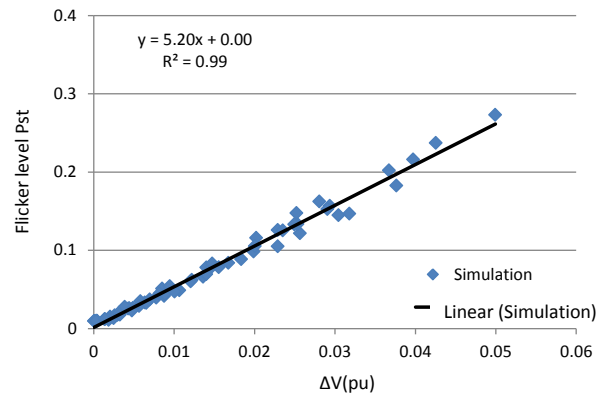
(c) $T_p = 9$ s



(e) $T_p = 13$ s



(d) $T_p = 11$ s



(f) $T_p = 15$ s

Fig. 6. Flicker level P_{st} versus maximum voltage difference ΔV for different peak periods T_p (for all impedance angles Ψ_k and all significant wave heights H_s).

terms of flicker level, to a real voltage profile $v(t)$ defined as

$$v(t) = V \sin(\omega_g t) \quad (12)$$

where ω_g is the grid radian frequency equal to $2\pi \times 50$ Hz. This latter voltage profile is composed of several sinusoidally-modulated voltage components of different amplitudes, phases and frequencies. Concerning the equivalent voltage profiles $v_{eq}(t)$, they are defined as

$$v_{eq}(t) = \frac{1}{2} \Delta V_{eq} \sin(2\pi t/T) \sin(\omega_g t) \quad (13)$$

In the case where the amplitude ΔV_{eq} of a sinusoidally-modulated voltage profile is equal to the maximum voltage difference ΔV of the real voltage profile, then

$$\frac{P_{st}}{\Delta V} = \frac{P_{st}}{\Delta V_{eq}} = a \quad (14)$$

In other words, the sinusoidally-modulated voltage profile $v_{eq}(t)$ induces the same flicker level P_{st} than the real voltage profile $v(t)$ provided that their amplitudes ΔV and ΔV_{eq} are equal. This means that a simple sinusoidally-modulated voltage profile can be used instead of a real voltage profile to estimate the flicker level for any impedance angle and for any wave height. This is a considerable advantage as real voltage profiles can only be obtained by means of sophisticated tidal turbine numerical models. However, the specific modelling of every turbine type proved to be a tremendous task, as experienced in the wind energy industry [18]. Hence, generic models are being developed in the marine energy industry in order to avoid this pitfall of specific modelling [19]–[21]. In this perspective, using a sinusoidally-modulated voltage profile can be considered as a relevant approach for estimating the flicker level induced by a tidal farm.

However, although the amplitude ΔV_{eq} is known (as equal to ΔV), the period T of the sinusoidally-modulated voltage profile still remains to be determined. Table II shows the period T_{eq} for which the flicker level P_{st} of the sinusoidally-modulated voltage profile $v_{eq}(t)$ is equal to this of the real voltage profile $v(t)$ when $\Delta V_{eq} = \Delta V$. The error in terms of flicker level is negligible as it never exceeds 0.01. Hence, as far as flicker analyses are concerned, this confirms that using a sinusoidally-modulated voltage profile is a sufficiently precise approach. Modelling this equivalent voltage profile requires determining the period T_{eq} , as well as the amplitude ΔV_{eq} based on the maximum and minimum values of the complex power $\mathbf{S} = P_{tot} + jQ_{tot}$ output by the farm. This method presents three main advantages. First, it avoids the need for sophisticated numerical models whose development is time-intensive, as mentioned earlier. Second, this limits the amount of information which the tidal device developer has to provide to non-commercially sensitive data (T_{eq} , $\max(S)$, $\min(S)$). Third, using this simple model can reduce considerably the computing time associated with flicker analyses: this can be extremely interesting in studies for which a high number of flicker analyses must be performed successively, e.g. optimisation studies.

Peak period T_p (s)	T_{eq}/T_p	T_{eq}/T_e
5	1.36	1.17
7	1.15	0.99
9	1.08	0.92
11	1.13	0.97
13	1.03	0.90
15	1.07	0.91

TABLE II
RATIOS OF PERIOD T (CHARACTERISING THE SINUSOIDALLY-MODULATED VOLTAGE PROFILE) TO THE ENERGY PERIOD T_e AND TO THE PEAK PERIOD T_p OF THE SEA-STATE

Peak period (s)		Error	
		$T = T_p$	$T = T_e$
5	max	0.10	0.19
	average	0.05	0.11
7	max	0.01	0.07
	average	0.00	0.04
9	max	0.03	0.03
	average	0.02	0.02
11	max	0.01	0.04
	average	0.01	0.02
13	max	0.03	0.01
	average	0.02	0.02
15	max	0.02	0.02
	average	0.01	0.01

TABLE III
MAXIMUM AND AVERAGE ERROR IN TERMS OF FLICKER LEVEL WHEN $T = T_p$ AND $T = T_e$

It must also be noted that period T_{eq} is relatively close to the temporal parameters typically used to characterise a sea-state (i.e. its energy period T_e or its peak period T_p), as shown in Table II and in similar fashion to a wave farm [15]. Table III shows the error in terms of flicker level when period T of the sinusoidally-modulated voltage profile is selected as equal to the energy period T_e of the sea-state or as its peak period T_p . The results indicate that the error is sufficiently small to use this approach as a preliminary estimation tool before more refined studies are performed.

IV. CONCLUSIONS

This paper has analysed the influence of sea waves on the quality of the electrical power generated by a tidal farm in terms of short-term flicker level P_{st} . The compliance of the tidal farm with the grid code requirements in terms of short-term flicker level was studied. Under the conditions considered in this paper, it was shown that the flicker level P_{st} induced by the tidal farm at the point of common coupling is unlikely to exceed even the most stringent limit found among a number of national grid codes. However, it reaches significant levels. Hence, in the case where the pre-connection flicker level is already significant, the grid connection of a tidal farm may lead the total flicker level at the point of common coupling to exceed the maximum allowed limit. Hence, the grid impact of a tidal farm in terms of flicker level must not be neglected.

This paper has also described a method for estimating the flicker level induced by a tidal farm. This method is based on modelling the voltage profile induced by the farm as a sinusoidally-modulated signal. Two approaches can be

considered: first, the period T of the sinusoidally-modulated voltage profile can be selected as equal to the energy period T_e or to the peak period T_p of the sea-state. This approach proved to be sufficiently precise for being used as a preliminary estimation tool. It was also shown that there exists a period T_{eq} for which the sinusoidally-modulated voltage profile is equivalent, in terms of flicker level, to the real voltage profile induced by the tidal farm. Hence, using such an equivalent voltage profile would avoid the need for tidal device developer or tidal farm manager to release commercially sensitive data. In addition, this approach could be used to develop simplified rules to be included in standards for instance.

Further work will focus on generalising this approach when a turbulent tidal flow is considered.

REFERENCES

- [1] EDF. Tidal farm of Paimpol-Bréhat, France. Accessed 9th February 2015. [Online]. Available: <http://energie.edf.com>
- [2] Verdant Power. RITE project. Accessed 9th February 2015. [Online]. Available: <http://www.verdantpower.com>
- [3] J. MacEnri, M. Reed, and T. Thiringer, "Influence of tidal parameters on SeaGen flicker performance," *Phil. Trans. R. Soc. A.*, vol. 371, no. 1985, 2013.
- [4] Z. Zhou, F. Sculler, J.-F. Charpentier, M. El Hachemi Benbouzid, and T. Tang, "Power smoothing control in a grid-connected marine current turbine system for compensating swell effect," *IEEE Trans. on Sustainable Energy*, vol. 4, pp. 816–826, 2013.
- [5] A. Saruwatari, D. Ingram, and L. Cradden, "Wave-current interaction effects on marine energy converters," *Ocean Engineering*, vol. 73, pp. 106–118, 2013.
- [6] P. Galloway, L. Myers, and A. Bahaj, "Quantifying wave and yaw effects on a scale tidal stream turbine," *Renewable Energy*, vol. 63, pp. 297–307, 2014.
- [7] B. Multon, "Marine renewable energy handbook," Wiley & Sons, 2013.
- [8] J. Falnes, *Ocean Waves and Oscillating Systems: Linear Interactions Including Wave-Energy Extraction*. Cambridge University Press, 2002.
- [9] L. Holthuijsen, *Waves in Oceanic and Coastal Waters*. Cambridge University Press, 2007.
- [10] B. Le Méhauté, *An Introduction to Hydrodynamics and Water Waves*. Berlin: Springer-Verlag, 1976.
- [11] L.-A. Dessaint and R. Champagne, "Permanent magnet synchronous machine," Matlab-Simulink model, R2014b.
- [12] M. Molinas, O. Skjervheim, B. Sørby, P. Andreasen, S. Lundberg, and T. Undeland, "Power smoothing by aggregation of wave energy converters for minimizing electrical energy storage requirements," in *Proceedings of the 7th European Wave and Tidal Energy Conference, Porto, Portugal, 2007*.
- [13] DiGSILENT PowerFactory. [Online]. Available: <http://www.digsilent.de/>
- [14] *Measurement and assessment of power quality characteristics of grid connected wind turbines, standard 61400-21, ed2.0, 2008*, IEC Std.
- [15] A. Blavette, D. O'Sullivan, R. Alcorn, T. Lewis, and M. Egan, "Impact of a medium-size wave farm on grids of different strength levels," *IEEE Trans. on Power Systems*, vol. 29, pp. 917–923, 2014.
- [16] AMETS test site. Accessed on 21st November 2014. [Online]. Available: www.seai.ie
- [17] *Flickermeter - Functional and design specifications, standard 61000-4-15, ed2.0, 2010.*, IEC Std.
- [18] Y. Coughlan, P. Smith, A. Mullane, and M. O'Malley, "Wind turbine modelling for power system stability analysis: A system operator perspective," *IEEE Trans. on Power Systems*, no. 3, pp. 929–936, 2007.
- [19] J. Khan, A. Moshref, and G. Bhuyan, "A generic outline for dynamic modeling of ocean wave and tidal current energy conversion systems," in *Power Energy Society General Meeting, 2009. PES '09. IEEE*, July 2009, pp. 1–6.
- [20] D. Mollaghan, D. O'Sullivan, A. Blavette, D. Cashman, R. Alcorn, M. Egan, and A. Lewis, "Generic dynamic modelling for grid integration of ocean energy devices," in *3rd International Conference on Ocean Energy, 6-10 October, Bilbao, Spain, 2010*.
- [21] S. Armstrong, D. Mollaghan, A. Blavette, and D. O'Sullivan, "An initialisation methodology for ocean energy converter dynamic models in power system simulation tools," in *47th International Universities Power Engineering Conference (UPEC), London, UK, Sept 2012*, pp. 1–6.